

5441

NUWC-NPT Technical Report 11,390
16 September 2002

Design Considerations in Reduced-Diameter Single-Mode Optical Fibers

Wilson K. S. Chiu
University of Connecticut

Gregory H. Ames
Marilyn J. Berliner
NUWC Division Newport

REFERENCE
LIBRARY USE ONLY



**Naval Undersea Warfare Center Division
Newport, Rhode Island**

Approved for public release; distribution is unlimited.



011390 001N

PREFACE

This report was prepared under Project No. A132102, "Fishline Array," principal investigator Marilyn J. Berliner (Code 2141). The sponsoring activity is the Office of Naval Research (Code 321SS).

The technical reviewer for this report was Daniel L. Baker (Code 2141).

W. K. S. Chiu performed this work under the American Society of Engineering Education (ASEE) Summer Faculty Fellowship Program sponsored by the Office of Naval Research.

Reviewed and Approved: 16 September 2002



Ronald J. Martin
Head, Submarine Sonar Department



REPORT DOCUMENTATION PAGE

Form Approved
OMB No. 0704-0188

Public reporting for this collection of information is estimated to average 1 hour per response, including the time for reviewing instructions, searching existing data sources, gathering and maintaining the data needed, and completing and reviewing the collection of information. Send comments regarding this burden estimate or any other aspect of this collection of information, including suggestions for reducing this burden, to Washington Headquarters Services, Directorate for Information Operations and Reports, 1215 Jefferson Davis Highway, Suite 1204, Arlington, VA 22202-4302, and to the Office of Management and Budget, Paperwork Reduction Project (0704-0188), Washington, DC 20503.

1. AGENCY USE ONLY (Leave blank)		2. REPORT DATE 16 September 2002	3. REPORT TYPE AND DATES COVERED	
4. TITLE AND SUBTITLE Design Considerations in Reduced-Diameter Single-Mode Optical Fibers			5. FUNDING NUMBERS A132102	
6. AUTHOR(S) Wilson K. S. Chiu Gregory H. Ames Marilyn J. Berliner				
7. PERFORMING ORGANIZATION NAME(S) AND ADDRESS(ES) Naval Undersea Warfare Center Division 1176 Howell Street Newport, RI 02841-1708			8. PERFORMING ORGANIZATION REPORT NUMBER TR 11,390	
9. SPONSORING/MONITORING AGENCY NAME(S) AND ADDRESS(ES) Office of Naval Research Ballston Centre Tower One 800 North Quincy Street Arlington, VA 22217-5660			10. SPONSORING/MONITORING AGENCY REPORT NUMBER	
11. SUPPLEMENTARY NOTES				
12a. DISTRIBUTION/AVAILABILITY STATEMENT Approved for public release; distribution is unlimited			12b. DISTRIBUTION CODE	
13. ABSTRACT (Maximum 200 words) A literature survey was performed to determine design considerations associated with the use of reduced-diameter (down to 40- μ m) optical fibers. Decreasing fiber diameter did not have a direct effect on cutoff frequency or numerical aperture. Bending loss is expected to increase due to the evanescent field escaping from the cladding. A possible solution to this issue is to use a depressed cladding fiber. Glass fiber tensile strength increased with fiber diameters less than 100 μ m. Several in-line methods and procedures are proposed to proof test the reduced-diameter fiber. However, fundamental limitations currently prohibit reliable quantitative lifetime predictions. Fiber-optic components will need to be modified in order to accommodate reduced-diameter designs.				
14. SUBJECT TERMS Fiber Optics Single-Mode Optical Fibers			15. NUMBER OF PAGES 22	
			16. PRICE CODE	
17. SECURITY CLASSIFICATION OF REPORT Unclassified	18. SECURITY CLASSIFICATION OF THIS PAGE Unclassified	19. SECURITY CLASSIFICATION OF ABSTRACT Unclassified	20. LIMITATION OF ABSTRACT SAR	

TABLE OF CONTENTS

	Page
LIST OF ABBREVIATIONS, ACRONYMS, AND SYMBOLS	ii
INTRODUCTION	1
LIGHT PROPAGATION AND THE CUTOFF FREQUENCY.....	1
NUMERICAL APERTURE	2
EVANESCENT FIELD.....	3
BENDING LOSS.....	4
DEPRESSED CLADDING	7
ATTENUATION	8
FIBER STRENGTH	9
FIBER COMPONENTS AND HANDLING	14
CONCLUSIONS.....	14
REFERENCES	15

LIST OF ILLUSTRATIONS

Figure	Page
1 Presence of Linearly Polarized Modes $LP_{\nu\mu}$ in a Step-Index Optical Fiber	2
2 Ratio of Power Carried in the Cladding to Total Power Carried by a Number of $LP_{\nu\mu}$ Modes as Functions of V	3
3 Normalized Field Distributions of the LP_{01} , LP_{11} , and LP_{02} Modes Versus the Normalized Radial Coordinate ($\rho = r/a$) in a Step-Index Fiber	4
4 Representative Optical Field Intensity Distributions of an 1.3- μm Optimized Step-Index Profile Single Mode Fiber at Two Different Wavelengths ($\lambda_2 > \lambda_1$)	6
5 Refractive Index Profile of (a) MC and (b) DC Step-Index Single-Mode Optical Fiber	7
6 Fundamental Loss Mechanisms in Silica Fibers.....	8

LIST OF ILLUSTRATIONS (Cont'd)

Figure		Page
7	Total Loss in Optical Materials.....	9
8	Optical Fiber Fracture Surface Showing the Typical Mirror-Mist-Hackle Pattern	10
9	Fiber Fracture Surface After Indentation with a 6.5- μm Crack.....	11
10	Dependence of Strength on Surface Area Tested and Glass Fibers Tested for Different Diameters (d) and Lengths (L).....	12
11	Static Fatigue of Silica Fiber with Different Coatings and Temperature Conditions.....	13

LIST OF ABBREVIATIONS, ACRONYMS, AND SYMBOLS

a	Core radius
DC	Depressed cladding
IR	Infrared
LP	Linearly polarized
MC	Matched cladding
MFD	Mode field diameter
NA	Numerical aperture
UV	Ultraviolet
V	Normalized frequency
Δ	Core-cladding refractive index difference
λ	Wavelength
ω_0	Modal spot size

DESIGN CONSIDERATIONS IN REDUCED-DIAMETER SINGLE-MODE OPTICAL FIBERS

INTRODUCTION

This report examines the reduction in diameter of single-mode optical fibers from the standard 125 μm to as small as 40 μm . Besides the challenging manufacturing issues that exist, a number of significant design considerations must be considered. Issues such as fiber strength, signal loss, and the handling of 40- μm fiber are addressed.

LIGHT PROPAGATION AND THE CUTOFF FREQUENCY

Single-mode optical fibers typically propagate with linearly polarized modes $LP_{\nu\mu}$ along the horizontal and vertical axes of the fiber. These two axes are orthogonally oriented with respect to the direction of propagation, which, in this case, is along the length of the fiber. The mode of light propagation in a fiber is a function of the core radius a , numerical aperture $NA \equiv \sqrt{n_1^2 - n_2^2}$, and wavelength λ as given by equation (1):

$$V = \frac{2\pi a}{\lambda} NA, \quad (1)$$

where V is the normalized frequency, and n_1 and n_2 are the refractive indices in the core and cladding, respectively. When $(n_1 - n_2) \ll 1$, the numerical aperture can be closely approximated by $NA = n_1 \sqrt{2\Delta}$, where $\Delta = n_1/n_2 - 1$. To retain a single-mode design, the normalized frequency must be kept below a particular value. The propagation behavior versus V for a step-index fiber is illustrated in figure 1.¹ In this figure, the LP_{01} mode solely propagates in the fiber until $V \approx 2.405$, at which point the LP_{11} mode appears.

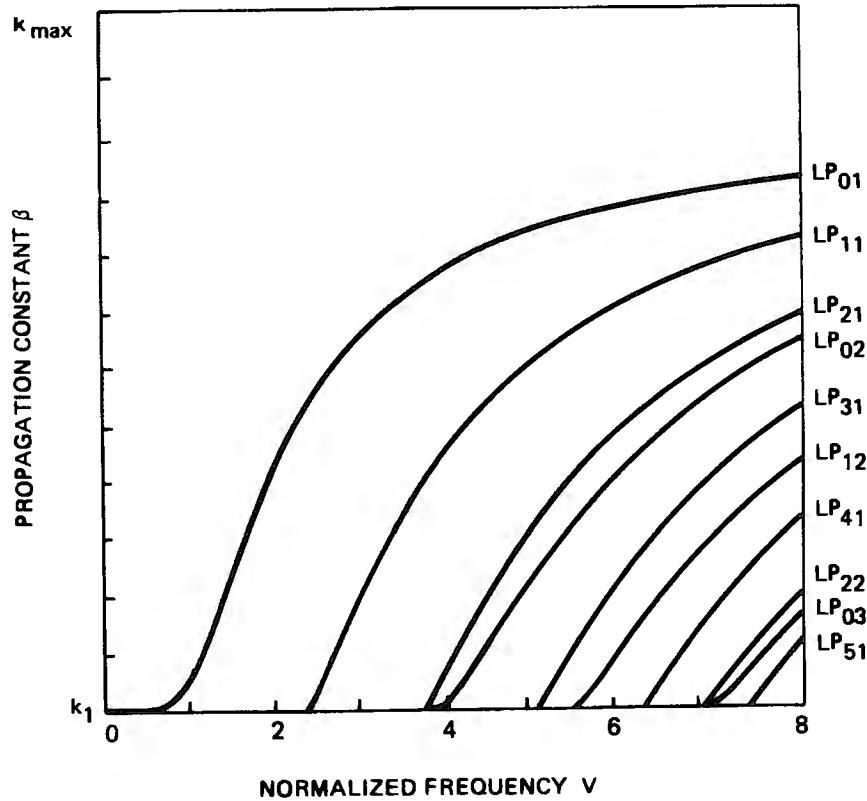


Figure 1. Presence of Linearly Polarized Modes $LP_{\nu\mu}$ in a Step-Index Optical Fiber (Tosco¹)

To keep the fiber design truly “single mode” (i.e., only the LP_{01} mode exists), a cutoff frequency of $V < 2.405$ must be maintained. But since V does not depend on the cladding radius, the proposed reduction in fiber diameter does not have a direct effect on cutoff frequency. However, V may be indirectly affected by changes in numerical aperture and wavelength.

NUMERICAL APERTURE

The numerical aperture is solely a function of the refractive index in the core and cladding $NA \equiv \sqrt{n_1^2 - n_2^2} = \sin\theta_i$, where θ_i is the angle of incidence from the normal fiber surface. Even though a direct relationship between NA and the cladding diameter does not exist, NA may be affected when a depressed cladding, dispersion compensation, or other design that may alter the refractive index difference between the core and the cladding material is considered.

EVANESCENT FIELD

It is commonly assumed that most of the signal in an optical fiber remains in the core. This assumption is partially true for single-mode fibers, and more so for multimode fibers. In single-mode fibers, 20 - 40% of the power is carried in the cladding due to an evanescent field generated between the core and cladding interface. The power distribution in the cladding depends on the normalized frequency, as illustrated in figure 2 from Miller and Chynoweth.² It is interesting to note that there is a gradual decay in cladding power for the LP_{01} mode, while cladding power rapidly decays with increasing V in higher-order modes. Beyond two core radii from the center, the cladding power drops to 1 - 5%, as shown in figure 3 from Tosco.¹ In summary, the cladding diameter needs to be greater than two core diameters to prevent significant signal leakage.

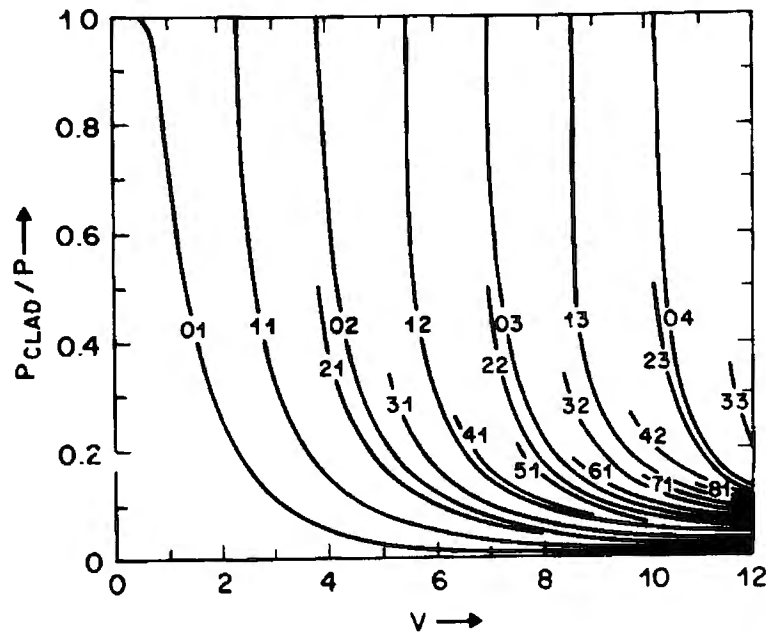


Figure 2. Ratio of Power Carried in the Cladding to Total Power Carried by a Number of $LP_{v\mu}$ Modes as Functions of V (Miller and Chynoweth²)

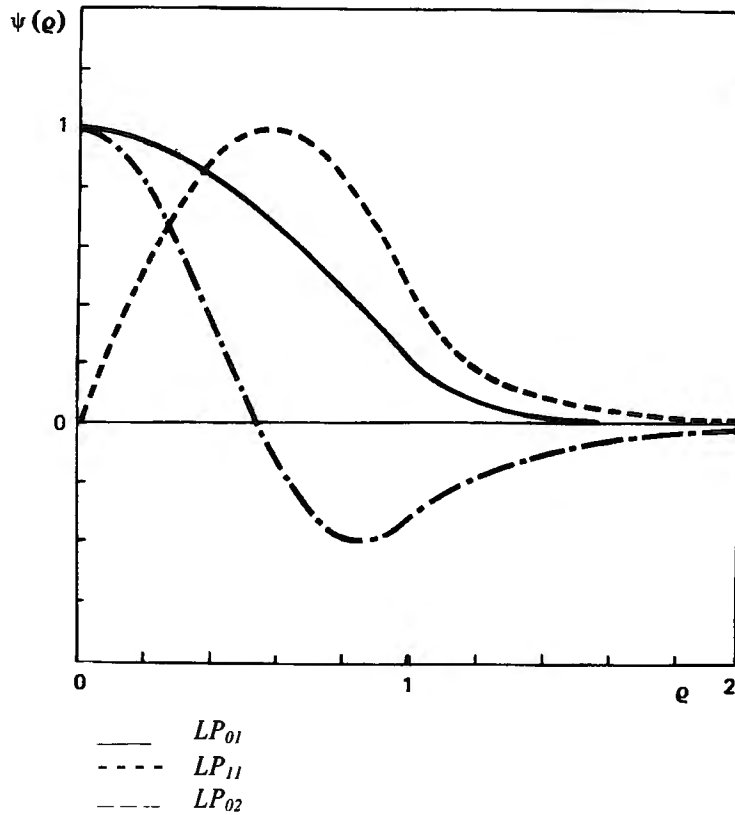


Figure 3. Normalized Field Distributions of the LP_{01} , LP_{11} , and LP_{02} Modes Versus the Normalized Radial Coordinate ($\rho = r/a$) in a Step-Index Fiber (Tosco¹)

BENDING LOSS

Signal loss due to bending can be classified into two types: *macro bending loss* and *micro bending loss*. Both losses are significant when the fiber diameter is reduced and must be considered in detail.

Macro bending loss is the most relevant external cause of attenuation and is due to macroscopic curvatures (namely, bends or loops) to which an optical fiber may be subjected during operation. Two loss mechanisms contribute to macro bending loss: transition loss and pure bending loss. Transition loss occurs in fiber sections following an abrupt change in curvature, while pure bending loss occurs when the curved fiber ceases to be a true guide structure. A rigorous study³ of macro bending loss considered the continuous superposition of Hankel functions to correctly represent cylindrical waves exiting the fiber. Matching this field to the field in the fiber core results in an expression for pure bending loss of

$$\gamma_B = FR^{-1/2} \exp(-AR), \quad (2)$$

where

$$F = \frac{\pi}{2aw^3} \left[\frac{\sqrt{V^2 - w^2}}{wK_1(w)} \right],$$

and

$$A = \frac{4}{3} \frac{n_2 - n_1}{n_2} \frac{w^3}{aV^2}.$$

Equation (2) indicates that macrobending losses depend very strongly on the radius of curvature R and other parameters F and A , representing the core-cladding refractive index difference, the core diameter a , the normalized frequency V , and the transverse propagation constant w , which rules the decay of the field in the cladding. Note that the finite dimension of the fiber cladding has not been taken into account in evaluating bending loss. This can become an important factor since power radiating into the cladding can couple back to the fundamental mode.

The analytical model presented in equation (2) for macrobending losses may be used to extract physical insight into macrobending losses in reduced-diameter fiber designs. It can be observed that loss increases exponentially with decreasing bend radius. To counteract this effect, the core-cladding refractive index difference ($\Delta = n_1/n_2 - 1$) can be increased. In other words, higher NA fiber can tolerate a smaller bend radius for a given amount of loss. This advantage can be used in the 40- μm design, where the core-cladding refractive index difference can be changed to reduce macrobending loss. This can be accomplished by increasing the core refractive index through higher doping levels, although this method can result in increased attenuation. An alternative is to use a depressed-cladding design to significantly increase NA , while keeping the core dopant concentration minimal. This issue is discussed further in the next section, "Depressed Cladding."

Microbending loss refers to signal loss due to very small, continuously varying bends of the fiber axis. The small bends, caused by jacketing or cabling processes, are randomly distributed. A detailed discussion by Tosco¹ explains that microbending losses depend not only on similar parameters as those observed in macrobending loss, but also on the modal spot size ω_0 . The modal spot size is related to the mode field diameter via $\text{MFD} = 2\sqrt{2} \omega_0$. Since $\omega_0 \sim \lambda/\sqrt{\Delta}$, shorter wavelength light or increased core-cladding refractive index difference can keep the modal spot size small, hence reducing microbending loss.

Figure 4 illustrates the effect of modal spot size on microbending loss. In this illustration, representative optical field intensities for two wavelengths, λ_1 and λ_2 , are superimposed on a step-index, single-mode fiber. Since $\lambda_2 > \lambda_1$, intensity distribution for λ_1 is more confined in the core, thereby reducing microbending loss into the cladding. Hence, small MFD and low microbending sensitivity can be achieved simultaneously.

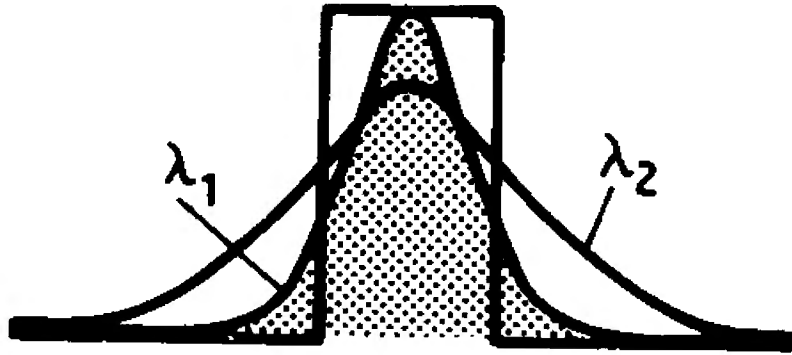


Figure 4. Representative Optical Field Intensity Distributions of an 1.3- μm Optimized Step-Index Profile Single-Mode Fiber at Two Different Wavelengths ($\lambda_2 > \lambda_1$)

Lazay and Pearson⁴ reported a comparison in bending loss between 125- μm - and 110- μm -diameter fiber. A simple experiment was conducted where the transmitted power through a short length of fiber (roughly 3 meters) was monitored as the radius of a single-circular loop in the fiber was decreased. A wavelength dependence on signal loss was observed for 110- μm -diameter fiber, with longer wavelength resulting in higher signal loss. Similar tests performed by Miya et al.⁵ for 110- μm -diameter fiber, however, did not exhibit this wavelength dependence. Lazay and Pearson proposed that the larger-diameter fiber did not have this long wavelength loss phenomenon for two reasons. First, the larger-diameter fiber is expected to be more robust and, thus, more resistant to externally induced curvature. Second, Miya's fibers were coated with a thick, soft silicone resin, which would cushion them from curvature-producing irregularities. Lazay's fibers were coated with a thin, hard, UV-cured epoxy-acrylate.

Lazay and Pearson⁴ also proposed several ways to control bending losses: (1) dope the substrate tube to match the cladding so that there is no leaky mode region; (2) use a large ratio of cladding to core diameter; and (3) choose Δ so that the optical field is better confined in the core.

In summary, bending losses arise in the form of macrobending loss and microbending loss. Both losses are sensitive to a number of design parameters, but limited information is available on loss dependence on cladding diameter. However, it has been shown that bending loss can be reduced by optimizing several parameters, including increasing the Δ and using a larger cladding-to-core diameter ratio. Depressed cladding fibers allow the designer to do just that.

DEPRESSED CLADDING

Two basic types of single-mode fibers are shown in figure 5. Figure 5a shows the matched cladding (MC) design, which has a typical MFD of about $10\ \mu\text{m}$ and a core-cladding refractive index difference (Δ) of about 0.11%. Figure 5b shows a depressed cladding (DC), with a typical MFD of about $9\ \mu\text{m}$ with relative index differences with respect to the cladding level Δ^+ and Δ^- of around 0.25% and 0.12%.¹ To decrease the refractive index in the cladding, fluorine is added to the DC fiber during the pre-form manufacture. DC fibers offer better bending resistance and tight mode confinement to the core, as discussed earlier in the “Bending Loss” section. An extension of DC fiber, called W fibers, selectively depresses the cladding refractive index in order to reduce waveguide dispersion. W fibers, a class of dispersion-flattened optical fibers, are designed for low loss in the 1.3- to 1.6- μm region, allowing for extensive and flexible frequency multiplexing. A detailed description of MC and DC fiber designs is presented in by Ainslie et al.⁶

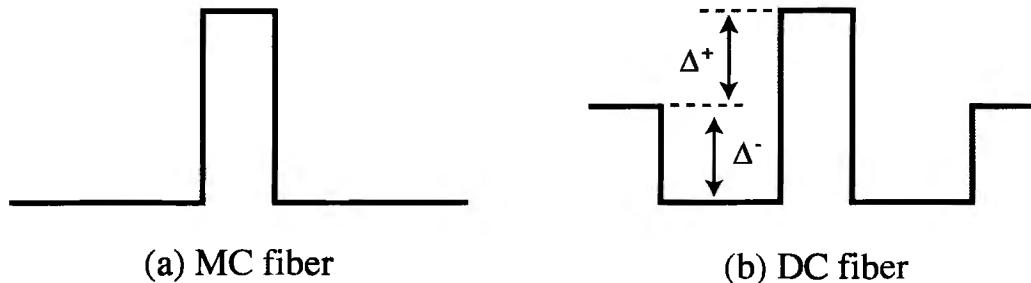


Figure 5. Refractive Index Profile of (a) MC and (b) DC Step-Index Single-Mode Optical Fiber

In summary, DC fibers should be considered on reduced-diameter fiber designs given their: (1) tight mode confinement to the core, (2) lower sensitivity to bending losses compared with the equivalent matched cladding fibers, and (3) reduction in waveguide dispersion using the W fiber design. However, DC fibers add significant complexities to the manufacturing process compared to MC fibers.

ATTENUATION

Light signal attenuation in optical fibers is the result of *intrinsic* and *extrinsic* factors. There are three intrinsic material mechanisms that cause attenuation: (1) absorption due to atomic electron interactions (UV absorption); (2) absorption due to light interactions with molecular vibrations (IR absorption); and (3) Rayleigh scattering. These three mechanisms, shown in figure 6 from Tosco,¹ result in a V-shaped curve with an anticipated loss minimum of around 1.55 μm . Nonlinear effects, such as Raman and Brillouin scattering, can cause a shift of the light wavelength. This occurs when high power is injected into an optical fiber.

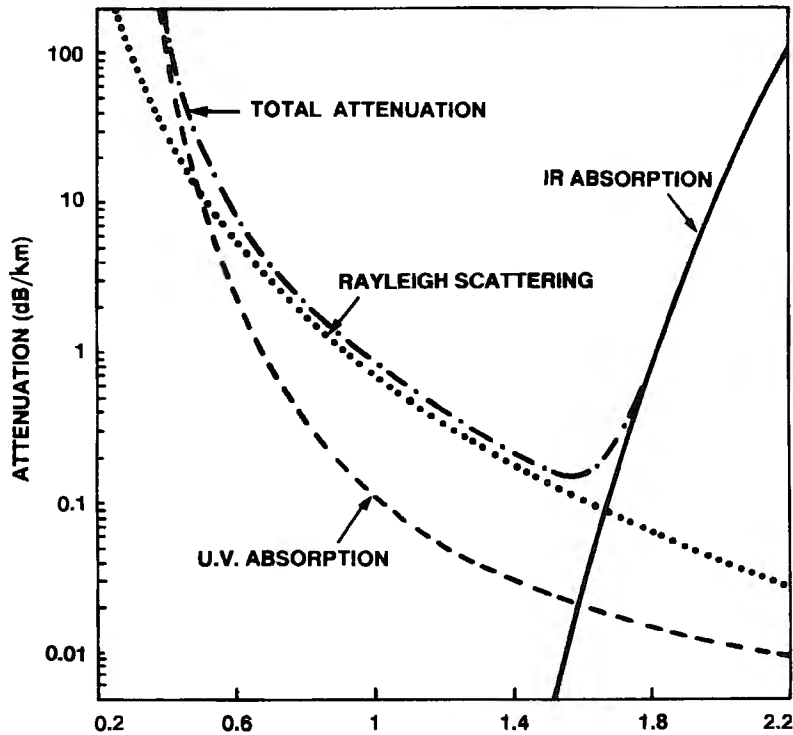


Figure 6. Fundamental Loss Mechanisms in Silica Fibers (Tosco¹)

Extrinsic attenuation factors include impurities in the fiber (e.g., transition metal ions, OH water radicals), waveguide imperfections such as material defects and stresses, and other factors arising in the material or fiber fabrication. There are also extrinsic factors associated with fiber deployment and environmental conditions, such as bending loss and exposure to harsh and chemically aggressive environments. A summary of total loss mechanisms from Tosco¹ is shown in figure 7.

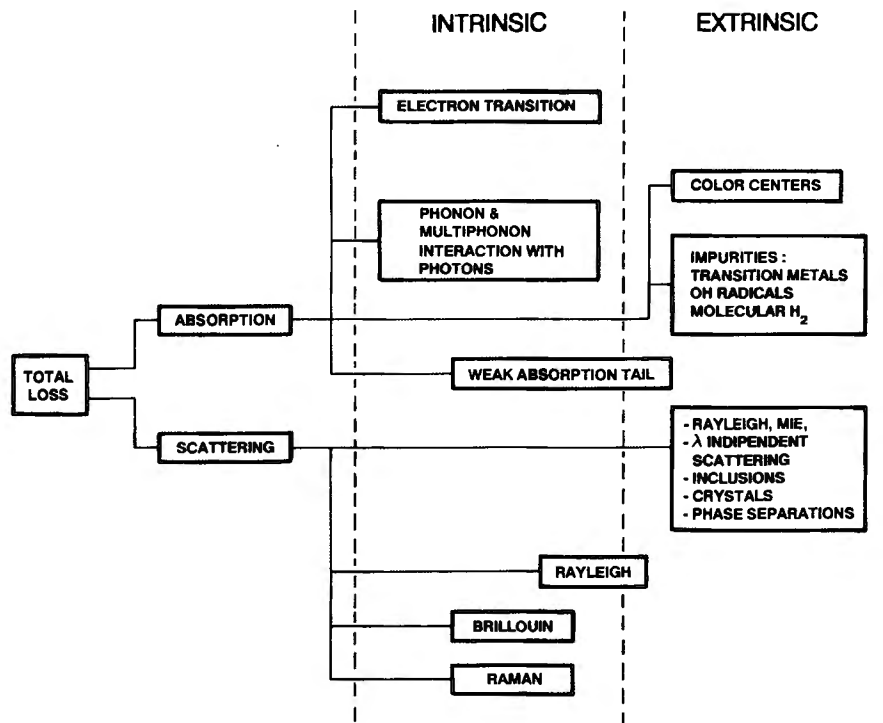


Figure 7. Total Loss in Optical Materials (Tosco¹)

Attenuation associated with the reduced-diameter optical fiber design shares similar concerns and design considerations with existing single-mode optical fibers. There are also additional considerations when DC is considered. Since the reduced-diameter design will have a smaller cladding thickness and the same diameter core, extrinsic attenuation due to bending loss and environmental conditions may be of greater concern. A thinner cladding may require larger cladding levels Δ^+ and Δ^- in which higher core doping concentrations may increase attenuation or other deleterious effects.

FIBER STRENGTH

Even though the theoretical strength of glass fibers may be estimated to be approximately 20 GPa by determining the cohesive bond strength of the constituent atoms,² most glass objects do not exhibit strengths anywhere near that value. Current commercial optical fiber tensile strength can exceed 5 GPa. Although high-strength fiber has been produced many times, it is not easy to achieve. Since fiber strength is significantly affected by surface quality and defects, all inputs to the drawing process must be controlled. Critical parameters of interest include bulk glass quality, glass surface quality, clean heat sources, coating processes, and coating applicators. Kurkjian et al.⁷ reviewed the progress in producing long lengths of high-strength optical fibers over the past 30 years. The authors describe insights that have been gained in

strength, aging (environmental degradation), and the combined behavior known as fatigue. Key technologies that allowed for the advance of high-strength fibers include manufacturing process improvements and the advent of new polymer and hermetic (inorganic and carbon) coatings. Even though coatings have allowed the industry to produce high-strength optical fibers, even the smallest defects in the fiber coating will cause failure. There are currently ongoing efforts to understand surface flaws and their contribution to fiber failure.

Recent developments have identified the importance of micron-sized flaws and their association to fiber failure. It is well known that tensile fractured glass materials exhibit a distinct mirror-mist-hackle pattern, as shown in figure 8 from Liao and Tan.⁸ Most fractures that exhibit such a pattern can be associated with the mirror region containing the crack-initiating surface flaw. Such observations can be used to identify the source and location of a flaw. Semjonov and Kurkjian⁹ demonstrated this by creating micron-sized flaws in glass fibers with a diamond cube-corner tip indenter. Their test sample, illustrated in figure 9, showed the same mirror-mist-hackle fracture pattern, with fiber tensile strength found to decrease significantly with the indentation size. Work is ongoing to determine the crack propagation and associated behavior for fiber failure.

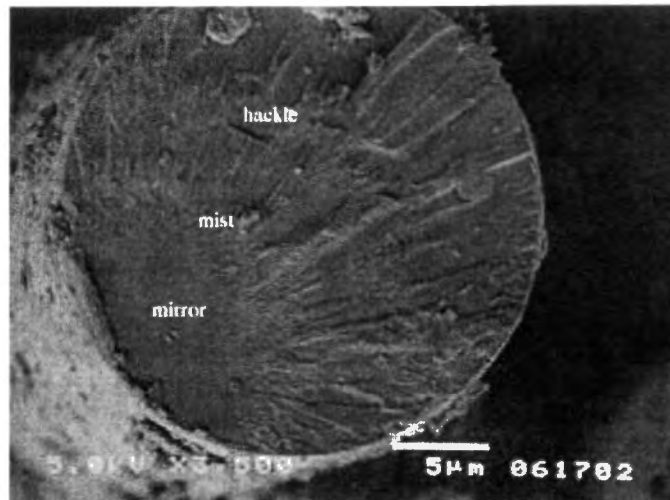


Figure 8. Optical Fiber Fracture Surface Showing the Typical Mirror-Mist-Hackle Pattern (Liao and Tan⁸)

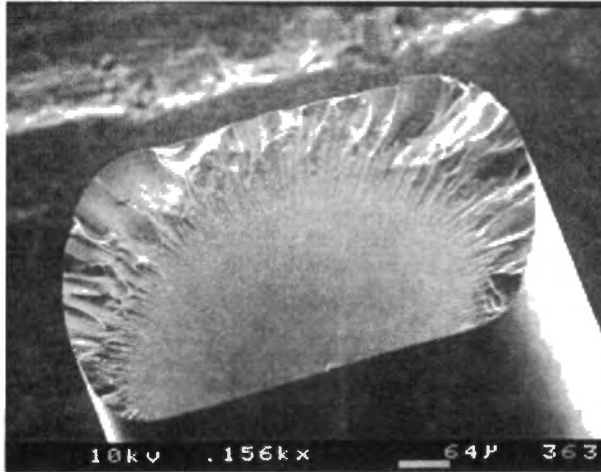


Figure 9. Fiber Fracture Surface After Indentation with a 6.5- μm Crack (Semjonov and Kurkjian⁹)

Glass fibers also display a sharp increase in strength with decreasing diameter when the gauge length is fixed, as reported in a comparison by Morley et al.¹⁰ Griffith¹¹ observed a similar phenomenon and postulated that surface flaws controlled fiber strength and that the probability of finding surface flaws increased with fiber surface area. Researchers, beginning with Otto,¹² then showed that the diameter dependence can be reduced or removed by drawing fibers at the same temperature. To allow comparison studies of length and diameter variations, Kurkjian¹³ proposed to convert diameter and length measurements into a surface area value. However, as figure 10 illustrates, Anderegg's data¹⁴ show that a substantial dependence of fiber strength on diameter still exists. Bartenev and Bovkunenko¹⁵ suggested that the effect of diameter changes on strength is due to diameter (d) and length (L) changes, as described by the following equations:

$$\sigma = A + B/d , \tag{3a}$$

and

$$\sigma = C/L^{1/n} . \tag{3b}$$

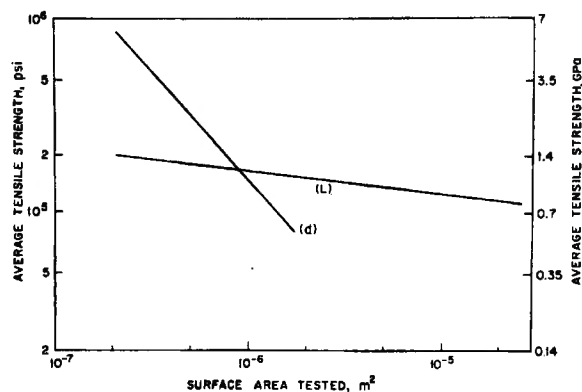


Figure 10. Dependence of Strength on Surface Area Tested and Glass Fibers Tested for Different Diameters (d) and Lengths (L) (Anderegg¹⁴)

This correlation is valid for fibers with diameters of less than 100 μm . Bartenev and Bovkunenko¹⁴ also postulated that this effect was caused by a quenched, oriented surface layer, but it was difficult to show this conclusively. Since the reduced-diameter effect is not found when the fiber diameter is greater than 100 μm , the fiber-optic industry has not considered this effect further.

Based on the limited studies on fibers of less than 100 μm in diameter, fiber strength has a significant dependence on fiber diameter. Even though the model reported in equation (3) yields an inverse relationship between fiber strength and diameter, a quantitative relationship between the two parameters is not available for fibers of less than 100 μm in diameter. For the proposed design, equal, if not increased, fiber strength should be evident for less than 100- μm -diameter fiber. The lower limit of d in equation (3) is unclear, however, and a quantitative value of fiber strength for 40- μm -diameter glass fiber is not available.

After drawing a reduced-diameter fiber, a reliable in-line proof test procedure must be developed for quality control. A considerable amount of information is available for in-line proof testing of 125- μm optical fiber (see, for example, Camilo and Matthewson,¹⁶ Donaghy and Dabbs,¹⁷ and Camilo¹⁸). Tensile proof testing is the preferred method over two-point bend testing because the latter method stresses a very small area of fiber.¹⁹ It would be difficult for two-point bend testing to detect large flaws that are typically isolated and distributed in many kilometers of fiber. For these reasons, tensile proof testing is the in-line test procedure of choice.

Reduced-diameter fibers may not be suitable for tensile testing, however. A tensile testing apparatus may have difficulty gripping the fiber without damaging it. If such conditions arise, an optional four-point bend testing technique may be used.^{20, 21} Four-point bend testing avoids the loading and gripping problems associated with other techniques and may be useful for relatively weak optical fibers.

Lifetime predictions are even more difficult to make, to the point that experts in the field do not believe that such predictions are currently possible. There is a significant set of problems

associated with lifetime predictions, as outlined by Kurkjian et al.⁷ When a fatigue curve ($\log \sigma$ versus $\log t$) is plotted for a particular sample, the slope of the curve must be constant or predictable in order to extrapolate the fatigue life of an optical fiber. However, a representative set of fiber samples from Kurkjian et al.⁷, shown in figure 11, demonstrates significantly different trends and behavior. Most noticeable is the onset of a “knee” in some samples. Several investigators have verified the presence of this fatigue knee. The kneeing phenomenon indicates a dramatic reduction of fiber strength, although this drop is unpredictable and has been shown to be strongly influenced by temperature, relative humidity, pH, and different types of coatings.

In summary, it is currently very difficult to predict the fatigue life of optical fibers since the stress corrosion susceptibility factor, which is inversely proportional to the gradient of the fatigue curve, is not constant during the fiber’s fatigue life. A possible solution is to remove or delay the knee through the use of hermetically or environmentally stable coatings, but significant research still needs to be done in this area.

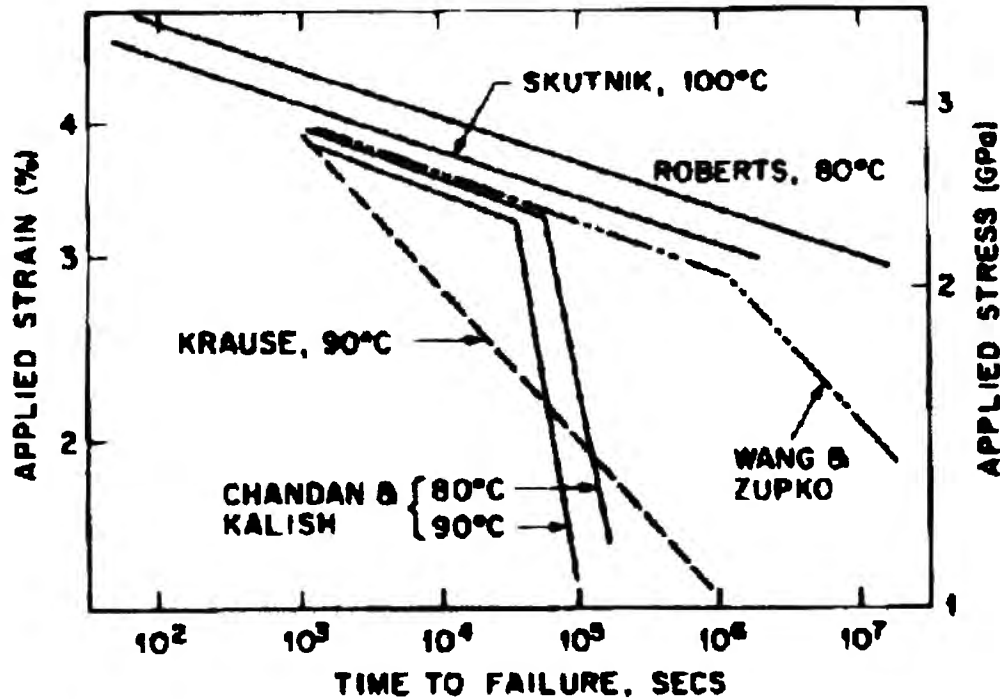


Figure 11. Static Fatigue of Silica Fiber with Different Coatings and Temperature Conditions (Kurkjian et al.⁷)

FIBER COMPONENTS AND HANDLING

The fiber-optic industry has expended considerable effort to develop connectors, splices, cables, sources, detectors, and other components for a set of standardized optical fiber diameters. For example, mechanical and fusion splices rely on the cladding outer diameter in order to align the core. Sources and detectors are typically supplied with pigtails or connectors standardized to a common fiber diameter (e.g., 125 μm). The proposed transition to smaller-diameter fiber will, at best, require a comprehensive set of connector interface components. A new set of standards will need to be developed in the future.

The handling of small-diameter glass fibers is also of concern. About 15 years ago, AT&T considered 110- μm -diameter fiber but later converged to 125- μm fiber due to handling issues.^{22, 23} Users found it difficult to strip, polish, and handle small-diameter fibers.

CONCLUSIONS

A number of design parameters have been considered to determine the most significant obstacles in reducing single-mode optical fiber cladding diameter from 125 μm to 40 μm , while keeping the core diameter fixed. A survey of available literature indicated that decreasing the cladding diameter does not have a direct effect on cutoff frequency or numerical aperture. However, bending loss is expected to increase due to the thin cladding's inability to contain the evanescent field. A possible solution is to use a depressed-cladding fiber, although core doping should be minimized to reduce attenuation.

Glass fiber tensile strength was observed to increase with cladding diameters of less than 100 μm . This would aid the proposed design, since a smaller diameter will essentially provide stronger fiber. This phenomenon is not well understood, however, and limited studies thus far have provided neither quantitative predictions nor a lower limit for the cladding diameter in equation (3). Several in-line proof test methods and procedures are suggested to characterize the reduced-diameter fiber. Due to fatigue kneeing and other limitations, it is currently very difficult to quantitatively predict an optical fiber's lifetime.

Fiber-optic connectors, splices, and other components will need modifications in order to properly align, connect, and splice reduced-fiber diameters to themselves or to standard fiber diameters. Handling of reduced-diameter fiber is also of concern.

REFERENCES

1. F. Tosco, *Fiber Optic Communications Handbook*, TAB Books, Blue Ridge Summit, PA, 1990.
2. S. E. Miller and A. G. Chynoweth, *Optical Fiber Telecommunications*, Academic Press, New York, 1979.
3. J. Sakai and T. Kimura, "Bending Loss of Propagation Modes in Arbitrary-Index Profile Optical Fibers," *Applied Optics*, vol. 17, no. 10, 1978, pp. 1,499-1,506.
4. P. D. Lazay and A. D. Pearson, "Developments in Single-Mode Fiber Design, Materials, and Performance at Bell Laboratories," *IEEE Journal of Quantum Electronics*, vol. QE-18, no. 4, 1982, pp. 504-510.
5. T. Miya, Y. Terunuma, T. Hosaka, and T. Miyashita, "Ultimate Low Loss Single Mode Fiber at 1.55 μm ," *Electronics Letters*, vol. 15, 1979, pp. 106-108.
6. B. J. Ainslie, K. J. Beales, C. R. Day, and J. D. Rush, "The Design and Fabrication of Monomode Optical Fiber," *IEEE Journal of Quantum Electronics*, vol. QE-18, no. 4, 1982, pp. 514-523.
7. C. R. Kurkjian, J. T. Krause, and M. J. Matthewson, "Strength and Fatigue of Silica Optical Fibers," *Journal of Lightwave Technology*, vol. 7, no. 9, 1989, pp. 1360-1370.
8. K. Liao and E. Y. M. Tan, "In Situ Tensile Strength Degradation of Glass Fiber in Polymer Composite," *Scripta Mater*, vol. 44, 2001, pp. 785-789.
9. S. L. Semjonov and C. R. Kurkjian, "Strength of Silica Optical Fibers with Micron Size Flaws," *Journal of Non-Crystalline Solids*, vol. 283, 2001, pp. 220-224.
10. J. G. Morley, P. A. Andres, and I. Whitney, "Strength of Fused Silica," *Physics and Chemistry of Glasses*, vol. 5, no. 1, 1964, pp. 1-10.
11. A. A. Griffith, "The Phenomena of Rupture and Flow in Solids," *Philosophical Transactions of the Royal Society of London, Series A: Mathematical and Physical Sciences*, vol. 221, 1920, p. 163.
12. W. H. Otto, "Relationship of Tensile Strength of Glass Fibers to Diameter," *Journal of American Ceramics Society*, vol. 38, 1955, p. 122.
13. C. R. Kurkjian, "Tensile Strength of Polymer-Coated Fibers for Use in Optical Communications," *Proceedings of the 11th International Congress of Glass*, 1977, p. 469.
14. F. O. Andereg, "Strength of Glass Fiber," *Industrial and Engineering Chemistry*, vol. 31, 1939, pp. 290-298.

15. G. M. Bartenev and A. N. Bovkunenko, "Various Factors Which Affect the Strength of Glass Fibers," *Zhurnal Tekhnicheskoi Fiziki*, vol. 26, 1956, p. 2,508.
16. G. M. Camilo and J. Matthewson, "Tensile Strength of High Speed Proof Tested Fiber Optics," *Proceedings of the IEEE International Microwave Optoelectronics Conference*, vol. 2, 1997, pp. 631-636.
17. F. A. Donaghy and T. P. Dabbs, "Subthreshold Flaws and Their Failure Prediction in Long-Distance Optical Fiber Cables," *Journal of Lightwave Technology*, vol. 6, no. 2, 1988, pp. 226-232.
18. G. M. Camilo, "Optical Fiber Complete Cumulative Flaw Distribution," *Proceedings of the SBMO International Microwave Conference*, vol. 2, 1993, pp. 423-428.
19. G. M. Camilo, "Qualitative Comparison Between Two-Point Bending and Tensile Tests in Optical Fibers," *Proceedings of the IEEE International Microwave Optoelectronics Conference*, vol. 1, 1999, pp. 286-289.
20. G. J. Nelson, M. J. Matthewson, and B. Lin, "A Novel Four-Point Bend Test for Strength Measurement of Optical Fibers and Thin Beams – Part 1: Bending Analysis," *Journal of Lightwave Technology*, vol. 14, no. 4, 1996, pp. 555-563.
21. G. J. Nelson, M. J. Matthewson, and B. Lin, "A Novel Four-Point Bend Test for Strength Measurement of Optical Fibers, and Thin Beams – Part 2: Statistical Analysis," *Journal of Lightwave Technology*, vol. 14, no. 4, 1996, pp. 564-571.
22. C. R. Kurkjian, private communication with Wilson K. S. Chiu, 22 June 2001.
23. P. Kaiser, private communication with Wilson K. S. Chiu, 3 July 2001.

INITIAL DISTRIBUTION LIST

	No. of Copies
Office of Naval Research (ONR) (R. Elswick (Code 321))	1
Naval Research Laboratory (A. Dandridge)	1
Defense Technical Information Center	2
University of Connecticut, Storrs (W. Chiu)	5